Available online at www.sciencedirect.com

SciVerse ScienceDirect

Ceramics International 39 (2013) 6069–6076

CERAMICS
INTERNATIONAL

www.elsevier.com/locate/ceramint

Effect of ceramic bonding phases on the thermo-mechanical properties of Al_2O_3–C refractories

Boquan Zhu, Yuenan Zhu, Xiangcheng Li*, Fei Zhao

The State Key Laboratory Cultivation Base of Refractories and Ceramics, Wuhan University of Science and Technology, Wuhan 430081, China

Received 12 November 2012; received in revised form 9 January 2013; accepted 9 January 2013

Abstract

Ceramic bonding phases of non-oxide whiskers can enhance the hot strength and the thermal shock resistance of Al_2O_3–C refractories. In this paper, the effect of different metals on the microstructure and thermo-mechanical properties of Al_2O_3–C refractories has been investigated. Thermodynamic calculation of Al–Si–O–C–N systems shows that Al_4C_3, AlN, SiC and β-Sialon are stable at elevated temperature. AlN with the shape of short column can be generated in Al_2O_3–C refractories with metallic Al, which leads to high hot modulus of rupture (HMOR) and poor resistance to thermal shock. SiC whiskers formed in Al_2O_3–C refractories with metallic Si give rise to low HMOR and good resistance to thermal shock. When metallic Si and Al are added together in the refractories, β-Sialon ($z=2$) with plane structure can be generated under the action of catalyst (nano-sized Ni). The existence of the catalyst promotes the diffusion of Al and O in Si_3N_4 crystals and contributes to the generation of plane-shaped β-Sialon. The corresponding HMOR and residual cold modulus of rupture respectively increase to about 20 MPa and 10.3 MPa. The plane-shaped β-Sialon can significantly enhance both hot strength and thermal shock resistance of Al_2O_3–C refractories.

Keywords: Ceramic bonding phases; β-Sialon; Plane structure; Thermo-mechanical properties; Al_2O_3–C refractories

1. Introduction

Carbon in refractories has the advantages of nonwettability by molten slag, high thermal conductivity and low thermal expansion [1–3]. All these features give rise to Al_2O_3–C refractories with excellent physical and chemical characteristics at elevated temperature, such as high hot strength, good resistance to both thermal shock and slag, etc. Therefore, Al_2O_3–C refractories can withstand long-lasting and repetitive chemical corrosion and mechanical attack coming from both molten steel and slag. Nowadays, Al_2O_3–C refractoreis are widely used as functional elements like nozzles, well blocks, sliding gate plates and stoppers in the continuous casting process of steel production [4–7]. The function of these refractories is to control flow field and velocity, decrease the addtion of impurity and prevent the oxidation of molten steel.

Al_2O_3–C refractories typically consist of corundum aggregate (larger than 0.088 mm) and the fine powder of matrix (smaller than 0.088 mm). The matrix usually contains corundum powder, graphite, anti-oxidant, binders and so on. The role of the matrix is to interlink coarser particles of the material. So the properties of the matrix could determine the density and mechanical strength of the refractories at room and high temperature. However, the matrix consisting of fine powder is often porous, fragile and easily eroded. When Al_2O_3–C refractories are attacked by molten liquids, the cracking and spalling will firstly occur in the matrix and ultimately deteriorates the comprehensive properties of the refractories. In order to enhance the properties of the matrix, the researchers usually added metals into the matrix as anti-oxidants because these metals can form ceramic bonding phases of SiC and AlN. The ceramic bonding phases, often taking on one dimensional structure, would reinforce the matrix and enhance the hot strength of Al_2O_3–C refractories through tightly interlinking the particle of corundum and graphite.

---

*Corresponding author. Tel.: +86 27 68862616.
E-mail address: lixiangcheng@wust.edu.cn (X. Li).

0272-8842/$ - see front matter Crown Copyright © 2013 Published by Elsevier Ltd and Techna Group S.r.l. All rights reserved.
http://dx.doi.org/10.1016/j.ceramint.2013.01.024

The usual additive in the matrix is metallic Si and Al, which will respectively form β-SiC whiskers and Al_4C_3 or AlN whiskers as the ceramic bonding phase at a high temperature. These ceramic whiskers would be in-situ generated at a high temperature under different conditions and play different roles during service [1,4,8,9]. For example, Fan et al. [6,10] found that metallic Si in Al_2O_3–C refractories would form SiC particles and SiC whiskers. The former are synthesized from the reaction between metallic Si and carbon black, while the latter are produced from the reaction between graphite flake and derivative carbon pyrolyzed from phenolic resin. The formation of much more curved SiC whiskers can enhance the hot strength for Al_2O_3–C refractories. Roungos and Aneziris [4] and Roungos et al. [5]also found that crystalline β-SiC whiskers in Al_2O_3–C refractories can be formed at 1400 °C. Yamaguchi [11] reported that metallic Al in Al_2O_3–C refractories could produce Al_4C_3 whiskers, which result in higher bending strength than that of alumina carbon refractories with metallic Si [12]. Based on thermodynamic calculation and growth mechanism of SiC whiskers [1,4,6,12], it is indicated that the silica added in samples will react with CO(g) to produce SiO(g). Then SiO(g) can easily react with CO(g) and is turned into SiC whiskers at a lower temperature. Meanwhile, because some metallic Al is consumed in the process of the reduction of silica, the decrease of aluminum carbide and existence of AlN could improve the hydration resistance of Al_2O_3–C slide gates [6,7,10–12].

In recent years, much effort has been directed to the further improvement of thermal shock resistance of Al_2O_3–C refractories through the modification of ceramic bonding phases. The greatest progress is in the development of β-Sialon whisker reinforcement in this system. β-Sialon is represented by the formula $Si_{6-Z}Al_ZO_ZN_{8-Z}$ ($Z=0$–4.2), which is also considered as the substitution of x Al–O groups for x Si–N groups in β-Si_3N_4 [13–18]. Compared with other ceramic whiskers (SiC, Si_3N_4, AlN, Al_4C_3, etc.), β-Sialon has an advantage in thermal and mechanical porperties, such as good resistance to both thermal shock and corrosion by liquid melts, excellent oxidation resistance, high hot strength at elevated temperature and so on [14,15]. So the ceramic bonding phases of β-Sialon whiskers could improve the high temperature properties of Al_2O_3–C refractories significantly. Li et al.[19] researched that in-situ synthesis of O-Sialon whiskers at 1500 °C could enhance the hot strength of Al_2O_3–C refractories because the whisker could tightly interlink the particle and matrix. Yue et al. [20] and Yu et al. [21] found that β-Sialon whiskers can be formed in Al_2O_3–C refractories with anti-oxidant of Al and Si. The β-Sialon

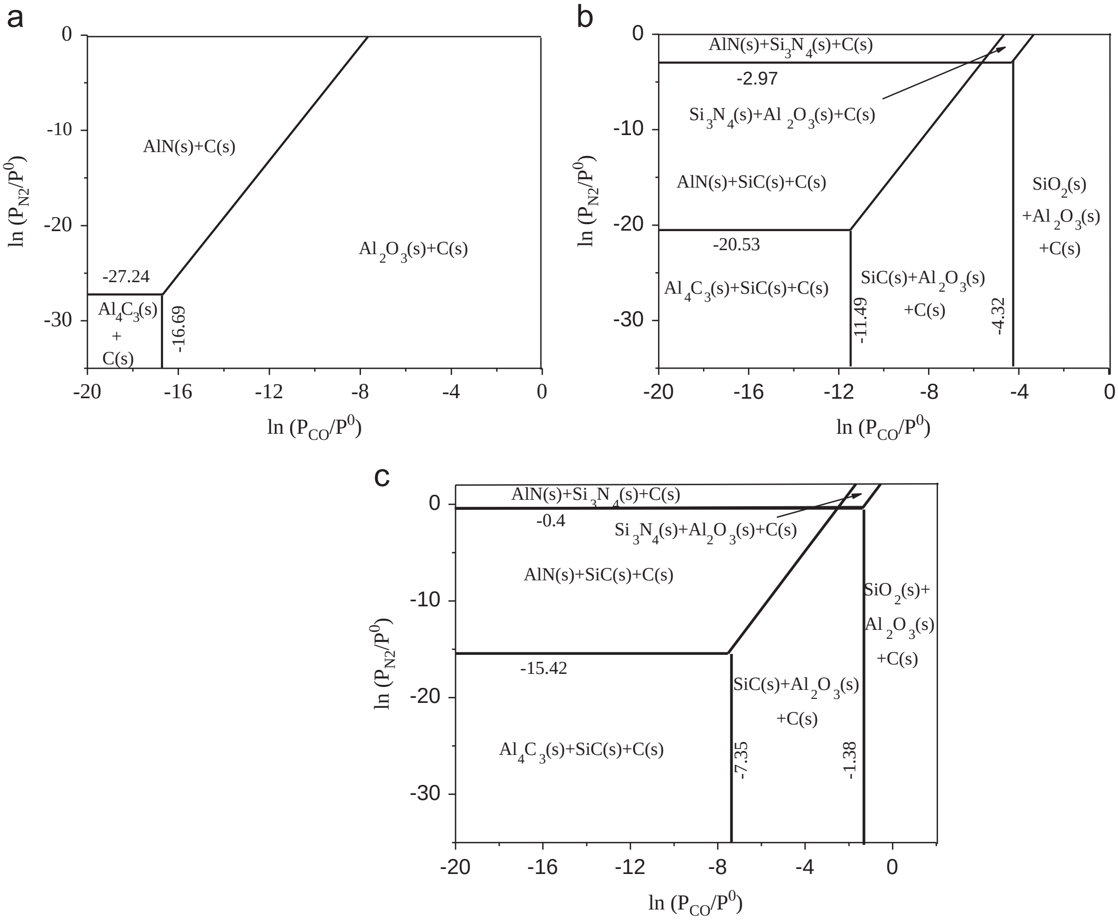

Fig. 1. Predominance area diagrams of the system Al–Si–O–C–N at (a) 1000 °C, (b) 1200 °C, and (c) 1400 °C.

whiskers would improve its hot strength greatly. They also found that the addition of β-Sialon based on bauxite could enhance the fracture strength up to 40 MPa at 1400 °C. Authors' previous work [22] also showed that β-Sialon bonded corundum slide gates have a fracture strength of 34.4 MPa at 1400 °C because the whiskers with large diameter improve its hot strength and oxidation resistance. At the same time, β-Sialon whiskers have been successfully synthesized in reducing atmosphere [23].

So in-situ synthesis of ceramic bonding phases is a key to the properties improvement of Al_2O_3–C refractories. Their morphology has a great influence on their comprehensive properties. The purpose of this paper is to study the formation mechanism of ceramic bonding phases with different morphologies, especially plane-shaped β-Sialon in Al–Si–O–C–N systems. Meanwhile, the effect of the ceramic bonding phases on the thermo-mechanical properties of Al_2O_3–C refractories has been studied.

2. Experiments

Coarse particles and fine powder of white fused corundum (99.60 wt% Al_2O_3), reactive alumina powder (98.50 wt% Al_2O_3 and d50 = 0.7 μm) and natural flake graphite (95.00 wt% < 88 μm) were used as raw materials. Metallic Si (98.50 wt%) and Al (99.50 wt%) were used as anti-oxidants. Phenolic resin was used as binder. The detailed compositions for Al_2O_3–C refractories are shown in Fig. 1. In order to study the effect of ceramic whisker bonding phases on the properties of Al_2O_3–C refractories, additions of Si and Al were used. As shown in Fig. 1, sample A included Al as an anti-oxidant while sample B contained metallic Si. For sample C both Al and Si have been added. At the same time, nano-sized metallic Ni was used in this sample as a catalyst. Three samples were mixed homogenously and then pressed into bar shaped samples (25 mm × 25 mm × 150 mm) at 150 MPa. The pressed samples were cured at 200 °C for 24 h and then subsequently coked at 1000 °C, 1200 °C and 1400 °C for 3 h in reducing atmosphere (embedded in the graphite where the atmosphere contains 35% CO and 65% N_2). The phase composition and the microstructure of the coked samples were determined through X-ray diffraction (XRD, X'Pert pro) and scanning electron microscopy (SEM, Nova NanoSem 400) supported by energy dispersive spectroscopy (EDS, Pheoenix).

The cold modulus of rupture (CMOR) of the coked samples was measured using three-point bending test at ambient temperature. The thermal shock resistance (at reducing atmosphere) of the coked samples was evaluated with the method of water quenching. The coked samples were heated at 1100 °C for 0.5 h in reducing atmosphere and then put into the water at room temperature for 5 min. The samples were dried and their residual CMOR was determined after one thermal shock cycle. The hot modulus of rupture (HMOR) of the samples heated at 1400 °C was measured in reducing atmosphere using three-point bending test. The testing temperature was 1400 °C and the soaking time was 30 min.

3. Results and discussion

3.1. Thermodynamic analysis of Al–Si–O–C–N systems

Based on FactSage software, thermodynamic calculations for Al–Si–O–C–N systems were conducted. The possible reaction in this system and the corresponding Gibbs free energy in standard state are shown in Table 2.

It is shown that it is easier for metallic Al to react with surrounding atmosphere (C, N_2 and O_2) than metallic Si because the Gibbs free energy of reactions (3)–(5) is lower. The melting point of Si is 1410 °C and its carbonization or nitrogen cannot begin until the temperature increases to about 1000 °C. A predominance area diagram for the system Al–O–C–N is depicted in Fig. 1(a) for 1000 °C. It is revealed that AlN is stable when $\ln(P_{N2}/P^0)$ is larger than -27.24, which is satisfied for the reducing atmosphere caused by graphite embedding where $\ln(P_{N2}/P^0)$ is -0.43. Stability of Al_4C_3 necessitates an even lower partial pressure of nitrogen associated with a low partial pressure of carbon monoxide.

At 1200 °C and 1400 °C, metallic Si will react with other system components and the stable phase compositions are shown in the predominance area diagrams of Fig. 1(b) and (c). SiC will be stable at 1400 °C when $\ln(P_{N2}/P^0) < -0.4$ and $\ln(P_{CO}/P^0) < -1.38$. For higher nitrogen partial pressure Si_3N_4 will be stable. This shows that a relatively high partial pressure of nitrogen would be needed for silicon nitride formation, which might not be achieved when the partial pressure is decreased by formation of aluminum nitride. The formation of β-Sialon from the nitrides together with alumina is shown in the following formula [13–16]:

$$(6-Z)Si_3N_4 + ZAl_2O_3 + ZAlN \rightarrow 3Si_{(6-Z)}Al_ZO_ZN_{(8-Z)}$$
$$\Delta G^0 = -778,370 + 392.12T\ (J)\ (Z = 2) \qquad (1)$$

The Gibbs free energy of reaction (1) at 1200 °C and 1400 °C is 200.78 kJ and −122.35 kJ, respectively, which is

Table 1
Experiment design of Al_2O_3–C refractories (wt%).

Samples	White fused corundum		α-Al_2O_3	Flake graphite	Anti-oxidant		In addition	
	3–0 mm	0.074 mm			Al	Si	Phenolic resin	Catalyst
A	65	22	6	4	3	–	4	–
B	65	22	6	4	–	3	4	–
C	65	19	6	4	3	3	4	0.5

Table 2
Reaction and Gibbs free energy for Al–Si–O–C–N systems.

no.	Chemical reaction	Gibbs free energy at standard state (J)	Temperature (K)
(1)	$C(s)+0.5O_2(g)\rightarrow CO(g)$	$\Delta G^\theta=-112{,}138-87.35T$	300–2000
(2)	$Al(s)\rightarrow Al(l)$	$\Delta G^\theta=10{,}268-10.859T$	933.45
(3)	$2Al(l)+1.5O_2(g)\rightarrow Al_2O_3(s)$	$\Delta G^\theta=-168{,}8477+327.45T$	933.45–2000
(4)	$Al(l)+0.5N_2(g)\rightarrow AlN(s)$	$\Delta G^\theta=-328{,}946+117.05T$	933.45–2000
(5)	$4Al(l)+3C(s)\rightarrow Al_4C_3{}^4(s)$	$\Delta G^\theta=-269{,}319+99.081T$	933.45–2000
(6)	$Si(s)+C(s)\rightarrow SiC(s)$	$\Delta G^\theta=-73{,}043+7.65T$	≤ 1685
(7)	$3Si(s)+2N_2(g)\rightarrow Si_3N_4(s)$	$\Delta G^\theta=-745{,}271+330.72T$	≤ 1685
(8)	$Si(s)+O_2(g)\rightarrow SiO_2(s)$	$\Delta G^\theta=-899{,}437+169.84T$	1140–1685

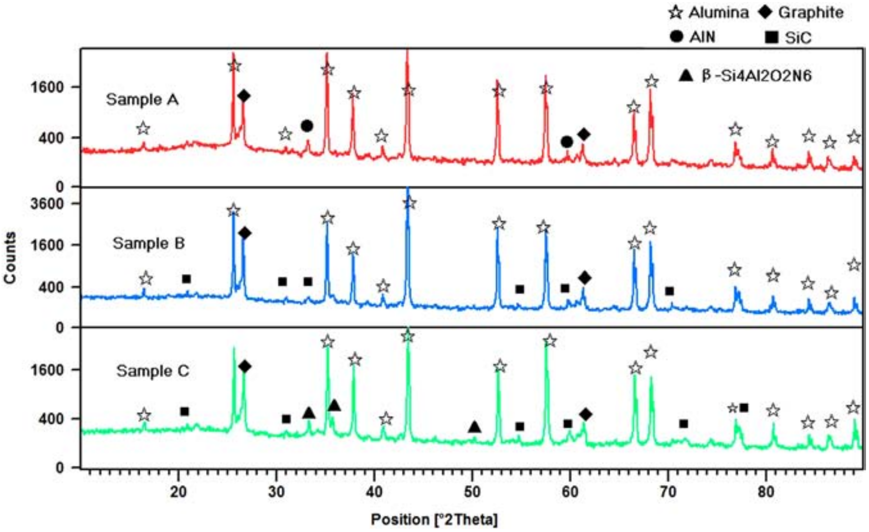

Fig. 2. XRD patterns of Al_2O_3–C refractories with different metals sintered at 1400 °C.

in good agreement with the report of Refs. [17,18]. So from thermodynamic calculation of Al–Si–C–N–O system, β-Sialon could be formed under reducing atmosphere when the temperature is raised to about 1400 °C.

3.2. Phase composition and microstructure of Al_2O_3–C refractories with different anti-oxidants

The XRD patterns of Al_2O_3–C refractories with different anti-oxidants are depicted in Fig. 2. It is shown that the major phases of three samples are corundum and graphite. Sample A with metallic Al as anti-oxidant has the peaks of AlN, while sample B with metallic Si has the peaks of SiC. Besides the phases of SiC, sample C with both metallic Al and Si has the peaks of β-$Si_4Al_2O_2N_6$. Thermodynamic calculation of Table 1 and Fig. 1 reveals that equilibrium partial pressures P_{N2} and P_{CO} of the coexisting phases AlN/Al_4C_3 and Si_3N_4/SiC, respectively, increases with rising temperature. For sample A, AlN could be generated at 1400 °C when the value of $\ln(P_{N2}/P^0)$ is larger than -0.43, which fits the condition of reducing atmosphere. It is also found that SiC is more stable than Si_3N_4 in sample B at this atmosphere according to the thermodynamic calculation. So in our experiment, SiC could be formed in sample B. When metallic Al and Si coexist in sample C, both SiC and β-$Si_4Al_2O_2N_6$ can be generated. It is worth noting that in theory β-$Si_4Al_2O_2N_6$ can be formed under reducing atmosphere from thermodynamic calculation of reaction (3). But many researchers [13–16] proved that it is difficult to generate β-Sialon because metallic Si easily reacts with carbon to form SiC and a high pressure of nitrogen is necessary for the formation of β-Sialon. In our experiment with low nitrogen pressure under reducing atmosphere, the existence of β-$Si_4Al_2O_2N_6$ results from the action of nano-sized Ni as catalyst. The catalyst introduced promotes the nitridation of metallic Si and helps to generate β-Sialon crystal structure [13,14].

The SEM for three samples is illustrated in Fig. 3. It can be seen that AlN (points 1 and 2 in Fig. 3) in sample A has the shape of both short-column and whisker while the peaks of O and C in the spectrum originate from the surrounding Al_2O_3 and graphite. The formation of AlN is followed by reactions (2) and (4). According to the morphology of AlN (point 1 in Fig. 3), the presence of liquid drops during formation of the whiskers is assumed. This reveals that the growth mechanism of AlN whiskers follows a vapor–liquid–solid model. This could change to a vapor–solid model when the liquid amount

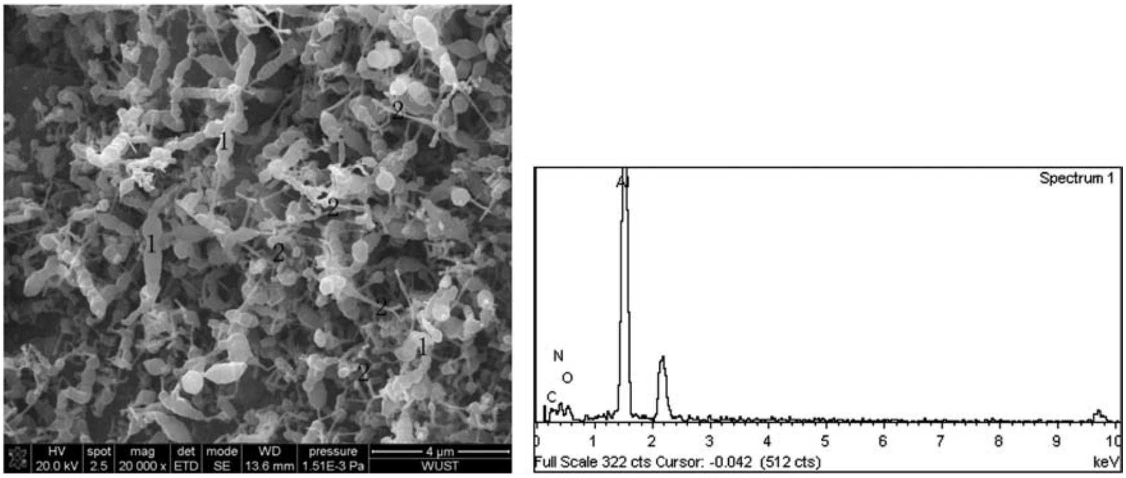

Fig. 3. SEM and EDS of Al_2O_3–C refractories with metallic Al (1: short column, 2: whisker).

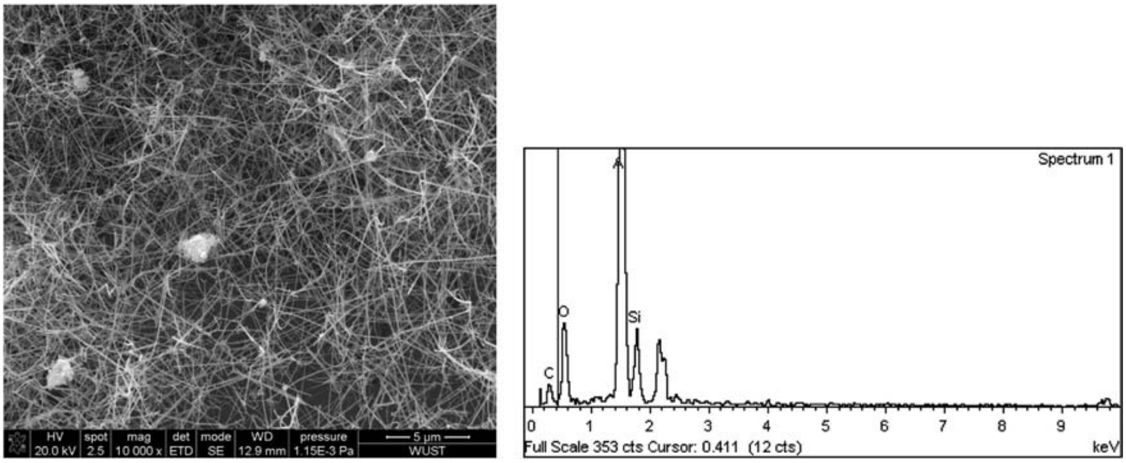

Fig. 4. SEM and EDS of Al_2O_3–C refractories with metallic Si.

is insufficient and bring about short-column morphology of AlN as shown by point 2 of Fig. 3. The corresponding reaction is given by $2Al_{(g)}+N_{2(g)}=2AlN_{(s)}$. The hexagonal structure of AlN also benefits the formation of short-column morphology. The results are consistent with the report of Li et al. [24] and Wang et al. [25], who also found that AlN with the same morphology as short-column type could be formed when the reaction system without Y_2O_3 addition lacks enough liquid at high temperature. Yang et al. [26] also found that using 5% Al, a suitable resin and some additives to the matrix promoted the formation of Al_3CON whiskers. But in our experiments, Al_3CON whiskers have not been found probably due to the presence of graphite, which is expected to cause a higher partial pressure of carbon monoxide.

For sample B with metallic Si as anti-oxidant, a large number of SiC whiskers (shown in Fig. 4) have been formed and the EDS reveals no nitrogen but peaks for Al and O originated from neighboring Al_2O_3. From the analysis of Table 1 and Fig. 1, it was found that SiC is easier to be formed than Si_3N_4.

Fig. 5 shows whiskers and plane structures formed in sample C with metallic Al and Si as anti-oxidants. XRD and EDS reveal that whiskers are composed of SiC and the planar structures are formed by β-Sialon. AlN was not found. It should be noted that β-Sialon occurs with planar shape but does not form whiskers. A vapor–liquid–solid reaction model is assumed for β-Sialon according to Eq. (1). With Ni acting as a catalyst the melting temperature of metallic Si can be decreased and the eutectic temperature is below 1200 °C. A first step of the reaction is the formation of a melt from Si and Al, later the dissolution of CO and AlO in this liquid, and finally the formation of SiC and β-$Si_4Al_2O_2N_6$ [13,16,27–29]. It is interesting to note that planar shape of β-$Si_4Al_2O_2N_6$ is preferred compared to one dimensional structures like whiskers and rods. The latter ones are believed to result from surface tension effects [27,29]. It is believed that the Ni catalyst promotes nitridation of Si, accelerates the diffusion of AlO into Si_3N_4, supports the β-Sialon formation and contributes to generation of planar structures. Without Ni acting as a catalyst Sialon growth will

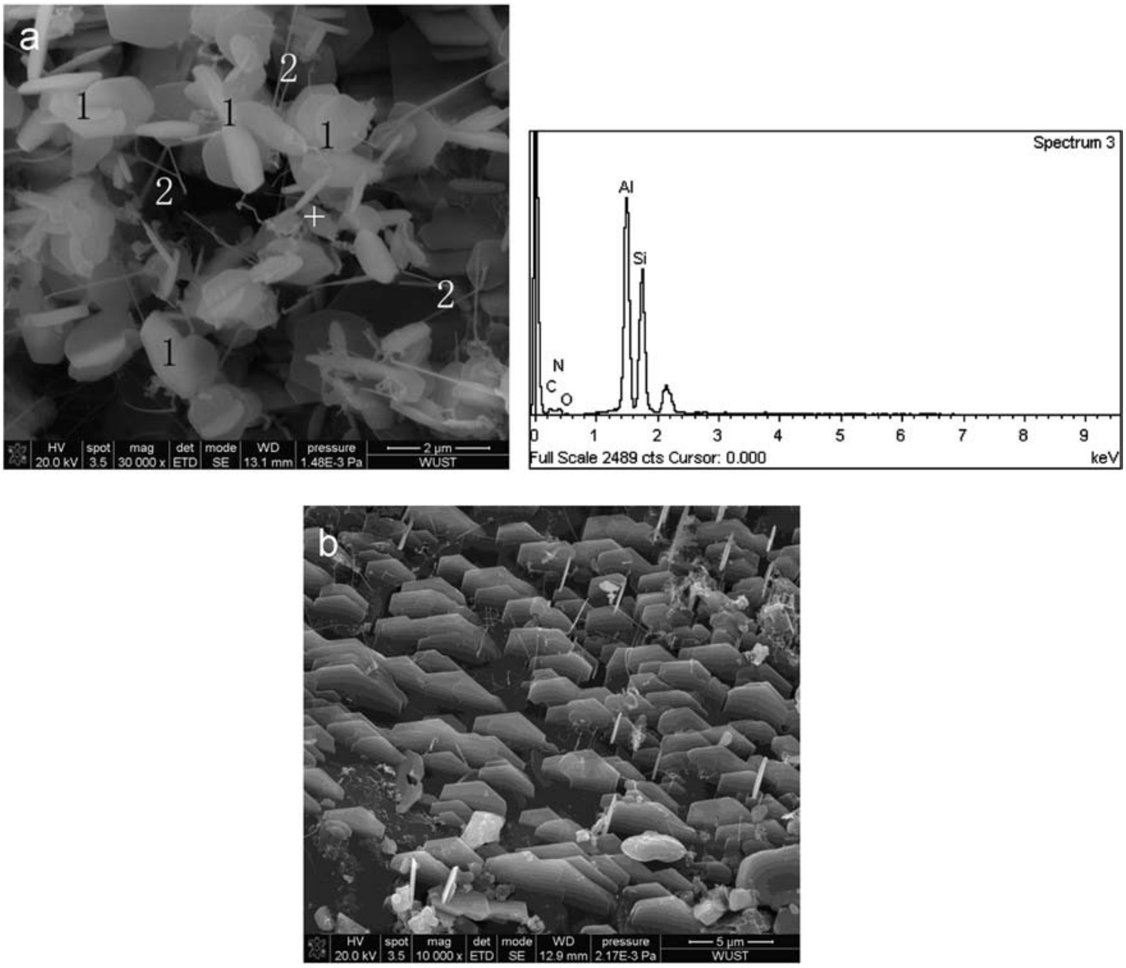

Fig. 5. SEM and EDS of Al_2O_3–C refractories with metallic Al and Si. (a) SEM and EDS of plane-shaped β-$Si_4Al_2O_2N_6$ (point 1) and SiC whiskers (point 2) and (b) SEM of β-$Si_4Al_2O_2N_6$ with plane structure.

be influenced by a gradient of the vapor concentration and the surface tension; this would result in whiskers [13,21,23].

3.3. *Strength of Al_2O_3–C refractories with different anti-oxidants*

The cold modulus of rupture (CMOR) for samples A–C sintered at different temperatures (1000 °C, 1200 °C and 1400 °C) is depicted in Fig. 6. CMOR of all samples increases with rising temperature due to the promotion of the sintering process and therefore enhanced the bonding. The increase of CMOR when rising the temperature from 1000 °C to 1200 °C for sample B is by far higher than that of samples A and C. This is due to the formation of silicon carbide, which does not take place at 1000 °C, but at 1200 °C. Compared with samples A and B, the CMOR of sample C at 1000 °C has doubled because the lower eutectic point of Al–Si would benefit the formation of ceramic bonding. At the same time, that would also help to improve the strength of refractories sintered at 1200 °C. When the sintering temperature is about 1400 °C, CMOR of sample C has the largest value of 23 MPa, compared with samples A and B.

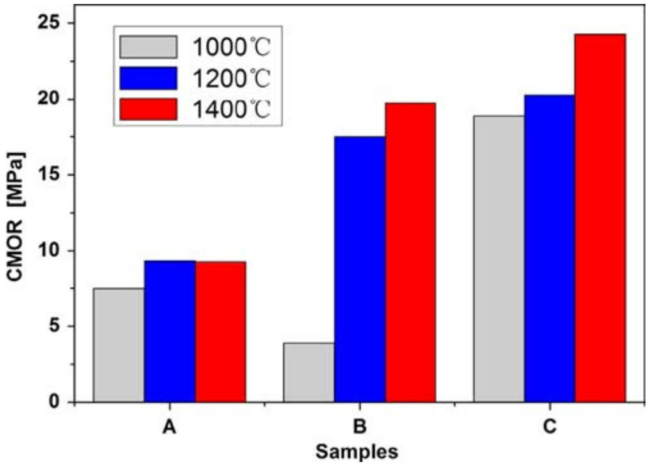

Fig. 6. Cold modulus of rupture (CMOR) of Al_2O_3–C refractories with different metals.

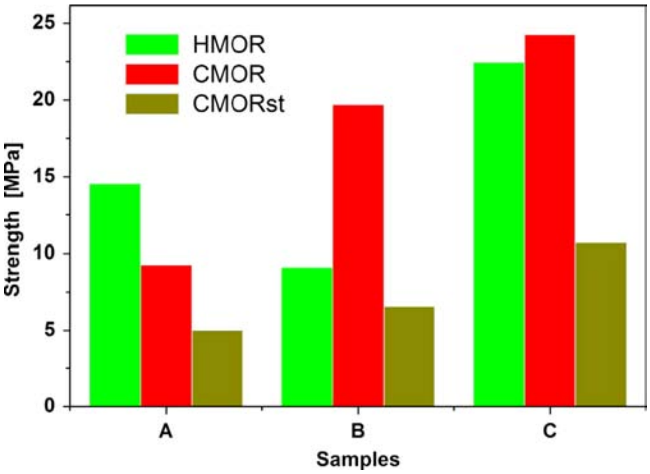

Fig. 7. HMOR (at 1400 °C), CMOR and CMORst of Al_2O_3–C refractories with different metals.

The hot modulus of rupture (HMOR) at 1400 °C and the change of CMOR for samples A, B andC after thermal shock at 1100 °C (with water quenching) are depicted in Fig. 7. At 1400 °C, the three samples have different bonding phases AlN, SiC and β-$Si_4Al_2O_2N_6$, correspondingly. This gives rise to the different HMOR. Sample A with the bonding phase of AlN whiskers and short-column shape has the HMOR of 15 MPa, while sample B with the bonding of SiC whiskers has the lowest HMOR of 8 MPa. The strength of AlN with one dimensional shape (short column and whisker) in sample A is higher than that of SiC whiskers in sample B, because the former has higher bonding strength with Al_2O_3. The result agrees with the report of Ref. [30]. As for sample C, β-$Si_4Al_2O_2N_6$ bonding phases with plate structure give rise to the highest HMOR of 20 MPa. It is believed that the reaction among Al_2O_3, Al, Si and N_2 to form β-Sialon enhances the bonding forces between the particles and the matrix and thereby increases the HMOR.

The residual CMOR (CMORst) after quenching specimens with a temperature of 1100 °C with water is depicted in Fig. 7. For carbon containing refractories, the thermal shock leads to large thermal stresses and oxidation, which would deteriorate the microstructure and strength. The CMORst of sample A has the lowest value of 4.3 MPa while that of sample C has the largest value of 10.3 MPa. The AlN bonding phase of sample A may hydrate during water quenching and thereby decrease the residual strength significantly. The high CMORst of sample C is attributed to the high bonding strength and the oxidation resistance of β-Sialon with planar structure. Upon oxidation of β-Sialon, mullite is expected to be formed, which also contributes to the ceramic bond.

4. Conclusions

(1) The thermodynamic analysis of the Al–Si–O–C–N system shows that Al_4C_3, AlN, SiC and β-Sialon may be stable depending on the partial pressures of nitrogen and carbon monoxide. Aluminum nitride with the morphology of short columns or whiskers can be generated in alumina carbon refractories with Al addition. SiC whiskers can be formed in the refractories with metallic Si. When metallic Si and Al are added in refractories with the addition of a Ni catalyst, β-$Si_4Al_2O_2N_6$ with plane structure and SiC whiskers can be formed.

(2) Alumina carbon refractories with AlN as ceramic bonding phases show high hot modulus of rupture (HMOR) and poor resistance to thermal shock. The refractories with SiC whiskers as ceramic bonding phases show low HMOR and good resistance to thermal shock. When the refractories are bonded by plane-shaped β-Sialon and SiC whiskers, their HMOR and residual cold modulus of rupture are 20 MPa and 10.3 MPa, respectively. The presence of β-Sialon with planar structure as a bonding phase significantly enhances the hot modulus of rupture and the thermal shock resistance.

Acknowledgment

Authors wish to appreciate the financial support of “973” project (2012CB722702), National Natural Science Foundation of China (Grant nos. 51174152 and 50904048), and Wuhan Chengguang project (201271031379).

References

[1] W.E. Lee, S. Zhang, Melt corrosion of oxide and oxide–carbon refractories, International Materials Reviews 44 (3) (1999) 77–104.

[2] X.C. Li, B.Q. Zhu, T.X. Wang, Electromagnetic field effects on the formation of MgO dense layer in low carbon MgO–C refractories, Ceramics International 38 (4) (2012) 2883–2887.

[3] X.C. Li, B.Q. Zhu, T.X. Wang, Effect of electromagnetic field on slag corrosion resistance of low carbon MgO–C refractories, Ceramics International 38 (3) (2012) 2105–2109.

[4] V. Roungos, C.G. Aneziris, Improved thermal shock performance of Al_2O_3–C refractories due to nano-scaled additives, Ceramics International 38 (2) (2012) 919–927.

[5] V. Roungos, C.G. Aneziris, H. Berek, Novel Al_2O_3–C refractories with less residual carbon due to nano-scaled additives for continuous steel casting applications, Advanced Engineering Materials 14 (4) (2012) 255–264.

[6] H.B. Fan, Y.W. Li, S.B. Sang, Microstructures and mechanical properties of Al_2O_3–C refractories with silicon additive using different carbon sources, Materials Science and Engineering A 528 (7-8) (2011) 3177–3185.

[7] X.C. Li, F. Zhou, B.Q. Zhu, The synthesis of B_4C/graphite composite powders and its effect on oxidation resistance for Al_2O_3–C refractories, Journal of the Chinese Ceramic Society 38 (6) (2010) 1070–1074.

[8] K. Sasai, Y. Mizukami, Reaction mechanism between alumina graphite immersion nozzle and low carbon steel, ISIJ International 34 (10) (1994) 802–809.

[9] J. Yu, A. Yamaguchi, Crystallization and oxidation behavior of carbon from phenolic resin in MgO–C and Al_2O_3–C refractories, Journal of the Ceramic Society of Japan 103 (3) (1995) 277–280.

[10] H.B. Fan, Y.W. Li, Y.P. Huang, Microstructures and mechanical properties of Al_2O_3–ZrO_2–C refractories using silicon, microsilica or their combination as additive, Materials Science and Engineering A 545 (2012) 148–154.

[11] A. Yamaguchi, Self-repairing function in the carbon-containing refractory, International Journal of Applied Ceramic Technology 4 (6) (2007) 490–495.

[12] A. Yamaguchi, Features and future development of the carbon-containing refractory, Key Engineering Materials 247 (2003) 239–244.

[13] V.A. Izhevskiy, L.A. Genova, J.C. Bressiani, F. Aldinger, Progress in Sialon ceramics, Journal of the European Ceramic Society 20 (13) (2000) 2275–2295.

[14] F.L. Riley, Silicon nitride and related materials, Journal of the American Ceramic Society 83 (2) (2000) 245–265.

[15] M. Vlasova, V.B. Vinokurov, O.N. Grigor'ev, A.D. Panasyuk, et al., Features of Sialon synthesis from kaolin, Materials Science and Engineering A 366 (2) (2004) 325–331.

[16] P.K. Panda, L. Mariappan, T.S. Kannan, Carbothermal reduction of kaolinite under nitrogen atmosphere,, Ceramics International 26 (5) (2000) 455–461.

[17] P. Dong, X. Wang, M. Zhang, M. Guo, W. Li, Thermodynamic study and syntheses of β-SiAlON ceramics, Science in China Series E 52 (11) (2009) 3122–3127.

[18] H. Mao, M. Selleby, Thermodynamic reassessment of the Si_3N_4–AlN–Al_2O_3–SiO_2 system—modeling of the SiAlON and liquid phases, CALPHAD 31 (2) (2007) 269–280.

[19] X. Li, C. Ke, N. Li, Alumina–carbon refractories strengthened by in-situ synthetic O–SiAlON whiskers, China's refractories 40 (6) (2006) 415–418.

[20] C. Yue, F. Ye, T. Li, X. Zhong, Y. Ren, Effects of β-SiAlON addition on properties of alumina–carbon refractories, China's refractories 40 (6) (2006) 440–442.

[21] J.K. Yu, W.B. Dai, S.P. Dai, Synthesis of Sialon–SiC composites and its application, Journal of Northeastern University 24 (9) (2003) 824–827.

[22] B.Q. Zhu, X.C. Li, C.J. Jin, β-Sialon bonded corundum materials and its application as sliding plate gate for continuous casting, Key Engineering Materials 280-283 (2005) 1683–1686.

[23] X.C. Li, B.Q. Zhu and F. Zhao, In-situ synthesis of SiC and β-$Si_3Al_3O_3N_5$ whiskers in alumina carbon based materials, Materials Science Forum, 745–746 (2012) 663–666.

[24] W.K. Li, B.L. Zhang, H.R. Zhuang, Preparation and growth mechanism of AlN whiskers by combustion synthesis with Y_2O_3 as additive, Journal of Materials Science 41 (2006) 2161–2163.

[25] H.B. Wang, D.O. Northwood, J. Han, Growth mechanisms for SiC–AlN solid soluteion crystals prepared by combustion synthesis, Journal of the American Ceramic Society 89 (2) (2006) 501–508.

[26] D. Yang, S. Yuan, M. Jiang, C. Ziiang, J. Zheng, D. Liang, Q. Zhang, Effect of matrix composition on physical properties of Al_3CON in-situ reaction reinforced corundum composite, Journal of Wuhan University of Technology-Materials Science Edition 23 (6) (2008) 927–931.

[27] C.L. Qin, G.W. Wen, X.Y. Wang, Ultra-long Sialon nano-belts: large-scale synthesis via a pressure enhanced CVD process and photoluminescence characteristics, Journal of Materials Chemistry 21 (16) (2011) 5985–5991.

[28] B. Zhong, X.X. Huang, G.W. Wen, Vapor phase synthesis of BN ribbons with Sialon ribbons as self-sacrificing templates, Materials Research Bulletin 46 (6) (2011) 970–974.

[29] Q. Yan, Q. Liu, Q.F. Liu, Synthesis of rod-like high-purity β-sialon powder by a novel carbothermal reduction–nitridation method with a nanocasting procedure, Journal of the American Ceramic Society 93 (9) (2010) 2470–2472.

[30] J.L. Huang, J.M. Jih, Investigation of SiC–AlN: part II. Mechanical properties, Journal of the American Ceramic Society 79 (5) (1996) 1262–1264.